JOURNAL OF APPLIED ELECTROCHEMISTRY 24 (1994) 758–766

Cathodic behaviour of antimony (III) species in chloride solutions

H. K. LIN, X. WU, P. D. RAO

Mineral Industry Research Laboratory, University of Alaska Fairbanks, Fairbanks, Alaska 99775-7240

Received 18 December 1992; revised 17 September 1993

Cathodic copper is easily contaminated by antimony in copper electrowinning from chloride solutions even when the antimony concentration in the electrolyte is as low as 2 p.p.m. Reduction potential measurements of copper and antimony species indicate that electrodeposition of antimony is unlikely unless copper concentration polarization exists near the cathode surface. A.c. impedance measurements and the effect of the rotation speed of the disc electrode indicate that the cathodic process mechanism for antimony is complicated. Both diffusion and chemical reactions occurring on the cathode surface supply the electrochemical active antimony species for the cathodic process. Reaction orders of the cathodic process with respect to antimony chloride, hydrogen and chloride ion concentrations are 2, −1 and −1, respectively. A proposed reaction mechanism for the process explains the experimental findings satisfactorily.

List of symbols

A	surface area (cm^2)
a_{o1}, a_1	constants
C	concentration ($mol\,cm^{-3}$)
D	diffusion coefficient ($cm^2\,s^{-1}$)
E	potential (V)
F	Faraday constant ($C\,mol^{-1}$)
f	frequency (s^{-1})
I	current (A)
i	current density ($A\,cm^{-2}$)
i_{d_s}	limiting diffusion current density due to the diffusion of species O from bulk to the electrode surface and then the subsequent Reactions 1 and 2 ($A\,cm^{-2}$)
i_{d_o}	limiting diffusion current density of species O ($A\,cm^{-2}$)
K	chemical equilibrium constant
k	rate constant (s^{-1})
n	number of electrons involved in the reaction
Q	charge (C)
Q_{dl}	charge devoted to double layer capacitance (C)
Q_f	total charge in the forward step of potential step chronocoulometry (C)
Q_r	total charge in reverse step of potential step chronocoulometry (C)
t	time (s)
v	sweep rate ($V\,s^{-1}$)

Greek symbols

Γ	amount of species adsorbed per unit area ($mol\,cm^{-2}$)
θ	fraction of adsorption sites on the surface occupied by adsorbate.
σ	ratio of rate constant defined in Equation 1
δc	thickness of reaction layer (cm)
δd	thickness of diffusion layer (cm)
τ	time (s)
τ'	modified time ($s^{1/2}$)
ν	kinematic viscosity ($cm^2\,s^{-1}$)
ω	angular velocity (s^{-1})

1. Introduction

Antimony is a common impurity in copper electrorefining and electrowinning from sulphate solutions. Usually this impurity is controlled within a range of 0.3–0.6 $g\,dm^{-3}$ in electrolytes. However, antimony solubility is 1.0–1.5 $g\,dm^{-3}$ in copper electrolytes containing 40–50 $g\,dm^{-3}$ Cu and 180–200 $g\,dm^{-3}$ free sulphuric acid at 323–333 K (50–60° C). Excess antimony has to be removed by decoppering electrolysis, hydrolysis, sulphide precipitation, solvent extraction, carbon adsorption or ion exchange [1–3]. Contamination of cathodic copper by antimony was discovered in copper electrowinning from cupric chloride solutions even when the antimony concentration in the electrolyte was as low as 2 p.p.m.

The effect of antimony on copper electrowinning from chloride electrolytes is more critical than that in sulphate electrolytes. Muir and Senanayake [4] showed that the reduction potential for antimony in chloride media lay close to the reduction potential of Cu(I). Therefore, antimony could contaminate cathodic copper in copper electrowinning from chloride solutions even at very low antimony levels. Only limited work has been reported on the investigation of antimony electrowinning technology in chloride electrolytes [5–8]. A cathodic reaction

0021-891X

mechanism was proposed as follows [8] without strong experimental evidence:

$$SbCl_3 + e^- \underset{k_{-1}}{\overset{k_1}{\rightleftharpoons}} SbCl_2(\text{adsorbate}) + Cl^-$$

$$SbCl_2(\text{adsorbate}) + e^- \xrightarrow{k_2} SbCl(\text{adsorbate}) + Cl^-$$

$$SbCl(\text{adsorbate}) + e^- \underset{k_{-3}}{\overset{k_3}{\rightleftharpoons}} Sb + Cl^-$$

$$SbCl_2(\text{adsorbate}) + e^- \underset{k_{-4}}{\overset{k_4}{\rightleftharpoons}} SbCl(\text{solid}) + Cl^-$$

In this work, cyclic voltammetry, a.c. impedance measurements, rotating disc technique and potential step chronocoulometry were employed to study the electrochemical behaviour of antimony. A reaction mechanism was then proposed to explain these experimental results.

2. Experimental procedures

All electrochemical measurements were obtained by using a model 273A potentiostat manufactured by EG & G Princeton Applied Research with a PS/2 computer. A modified H-type three-electrode cell with sintered-pyrex disc of fine porosity was used. A copper, platinum, glass–carbon or antimony electrode was used as the working electrode depending on the tests conducted. A calomel electrode with saturated KCl was used as the reference, and a platinum electrode as the auxiliary.

The working electrodes were pretreated by polishing with 0.05 μm Al_2O_3; soaking in 3 N HNO_3 and 3 N HCl solutions sequentially for 1 h (for platinum electrode); washing with 3 N HCl (for glass–carbon, Cu and Sb electrodes) and then washing with distilled water. This electrode pretreatment is completed immediately before starting each test.

The cell was located in a water bath, of which the temperature was controlled at 298 K (25° C) by a Dyna-Sense temperature controller.

High purity nitrogen was used for purging the electrolytes in the cell for 1 h before starting a test and for shielding atmosphere in the cell during the test.

All potentials reported were referred to the standard hydrogen electrode (SHE).

Cyclic voltammetry with various sweep rates was used as a convenient method for diagnosing if coupled chemical reactions were present. Potential step chronocoulometry was used for the measurement of amounts of adsorbate on the surface of the electrode. Reaction orders of the reactants were determined under the conditions of negligible concentration polarization of electrochemically active species with a high rotation speed of the disc electrode. A.c. impedance measurements were employed with an a.c. amplitude of 5 mV and the d.c. potential of the reduction potential of antimony (III) chlorides.

Except for the a.c. impedance tests, *IR* compensation with positive feedback and low-pass filter were used.

All reagents used in these tests are of analytical grade.

3. Results and discussion

3.1. *Reduction peak potentials of antimony* (III) *and copper* (I)

The reduction peak potential of Cu(I) at the copper electrode is more positive than that of Sb(III), as indicated in Table 1. Therefore the Sb(III) reduction is unlikely under conditions of copper electrowinning from chloride electrolytes, containing more than 10 g dm^{-3} copper and less than 0.1 g dm^{-3} antimony, without some degree of copper concentration polarization near the cathode surface.

3.2. *Effect of sweep rate on antimony reduction*

Cyclic voltammetry was employed to investigate the effect of sweep rate v/V s^{-1}, on the electrochemical response of the antimony reduction.

As shown in Fig. 1, the peak potential of Sb(III) reduction, E_p, decreases with increase of the sweep rate, indicating that this electrochemical reaction is irreversible.

Nicholson and Shain [9] and MacDonald [10] have discussed the effect of v on current under various conditions. A dimensionless current function was used in mathematical expressions of the current and the figures of the peak current function, I_p against v have been established [9]. Under a condition of chemical reactions preceding an irreversible discharging step, the current function is proportional to $I/v^{1/2}$ thus a plot of $I_p/v^{1/2}$ against v resembles the plot of peak current function against v [9]. As presented in Fig. 2, the shape of curve in the plot of $I_p/v^{1/2}$ against v indicates that there is a chemical reaction followed by the subsequent electrochemical reactions in the Sb(III) reduction [9].

Table 1. Reduction peak potentials of Cu(I) *and Sb*(III) *chlorides*

Composition of electrolytes				*Electrode*	*Reduction peak potentials*	
Cu /g dm^{-3}	*Sb* /g dm^{-3}	H^+ /M	Cl^-_{total} /M		*Discharging species*	*Potential values* /V vs SHE
10	0	0	3.30	Cu	Cu(I)	+0.008
0	0.1	0.03	3.1	Cu	Sb(III)	−0.043

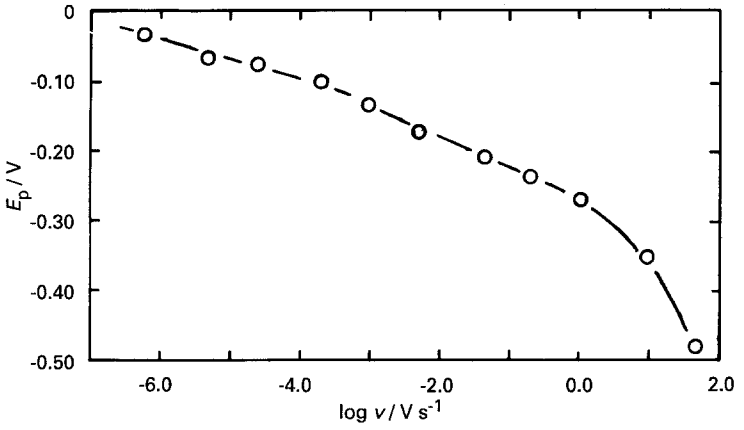

Fig. 1. Effect of sweep rate, v (V s^{-1}) on peak reduction potential with an antimony electrode. Composition of electrolyte: 1 g dm^{-3} Sb, 0.3 M HCl, and 3 M NaCl.

3.3. *A.c. impedance of antimony* (III) *chloride reduction system*

The Randles plot is useful in determining whether Warburg impedance is a significant component of the equivalent circuit model. An idealized Randles plot of Z' (real component of the impedance) against $f^{-1/2}$ (frequency) for a diffusion controlled system should be a straight line, with the intercept at $f^{-1/2} = 0$ equal to the electrochemical reaction resistance of the system plus the uncompensated ohmic resistance. In this study the reduction system of antimony (III) in the chloride solutions is found to be more complicated than a simple charge-transfer system. Figure 3 shows that the Warburg impedance is important only in higher frequencies and insignificant in lower frequencies. This is probably due to that in the lower frequencies, the electrochemical active species produced by the preceding chemical reactions on the electrode surface (usually named 'chemical sources') is significant. Hence, the supply of the electrochemical active species for the discharging reaction is not dominated by the diffusion of the species from the bulk solution.

3.4. *Effect of rotation speeds of disc electrode on antimony* (III) *reduction in chloride solutions*

When a rotating disc electrode (RDE) is employed in electrochemical measurements, plot of i against $\omega^{1/2}$, where i is current density and ω is angular velocity, is linear for a diffusion controlled process as indicated in Levich equation [11]. As the process is gradually changed to electrochemical reaction control with increase of the RDE speed, the curve will level off.

As shown in Fig. 4, the curve does not tend to reach the limiting diffusion current density even at the RDE speed of 8000 r.p.m. Also with the fact that the plot of $1/i$ against $1/\omega^{1/2}$ is linear (correlation coefficient = 0.99) (Fig. 5), these characteristics indicate that there is at least a chemical reaction preceding the discharge steps [12]. It may be worth noting that mathematically, in the plots of i against $\omega^{1/2}$ and $1/i$ against $1/\omega^{1/2}$, the linearity of one does not imply the linearity of the other under cases where the intercepts of y-axis are not zero. This is why $1/i$ against $1/\omega^{1/2}$ is linear (Fig. 5) while i against $\omega^{1/2}$ (Fig. 4) is not. Physically, it indicates that in addition to the diffusion of electrochemically active species from bulk to the electrode surface, 'chemical sources' exist. The mathematical formula of the relationship between $1/i$ and $1/\omega^{1/2}$ has been detailed under the case where 'chemical sources' exist [12].

Suppose the reactions are as follows:

$$S \underset{k_{-1}}{\overset{k_1}{\rightleftharpoons}} O \qquad (\sigma = k_{-1}/k_1) \tag{1}$$

$$O + ne^- \longrightarrow R_e \tag{2}$$

where S and O are the electrochemically inert and active species, respectively, R_e is the reaction product, and k_1 and k_{-1} are forward and backward reaction rate constants, respectively.

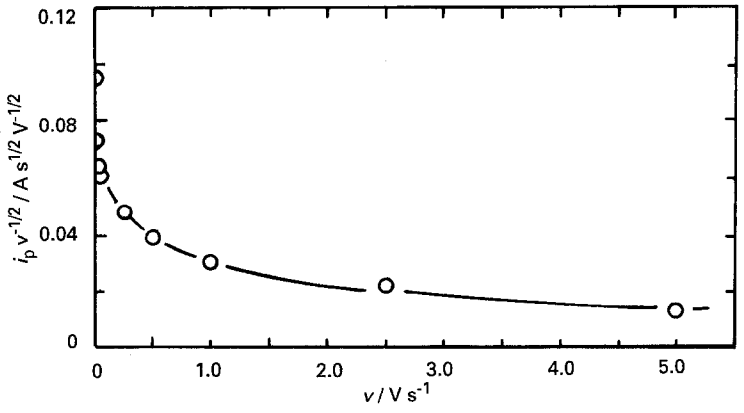

Fig. 2. Relationship between $I_p/v^{1/2}$ and v. Composition of electrolyte: 1 g dm^{-3} Sb, 0.3 M HCl and 3 M NaCl.

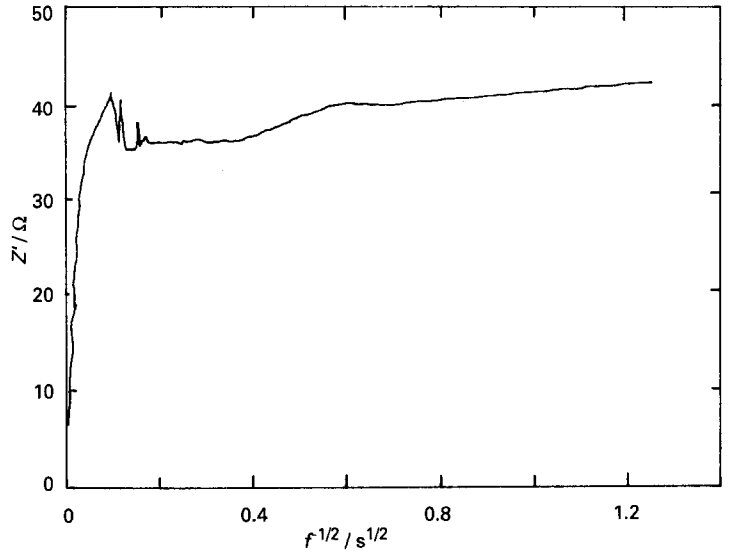

Fig. 3. Randles plot of Sb(III) chloride reduction system. Solution composition: 1 g dm^{-3} Sb, 0.3 M HCl, and 3 M NaCl. A.c. amplitude: 5 mV; d.c. potential: −0.0015 V vs SHE.

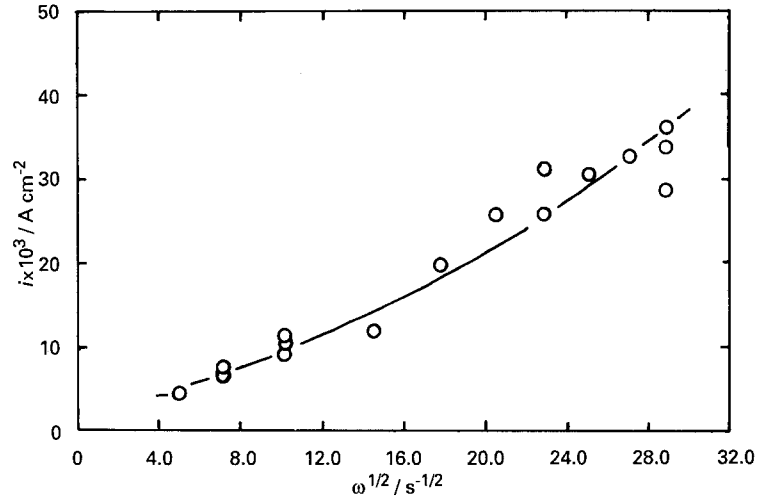

Fig. 4. The relationship between i against $\omega^{1/2}$ at rotating glasscarbon disc electrode and potential of −0.05 V vs SHE. Sweep rate: 1 mV s^{-1}. Composition of electrolyte: 1 g dm^{-3} Sb, 0.3 M HCl and 3 M NaCl.

Under the case of $\sigma \gg 1$, the following equation can be obtained through solving diffusion equations with a chemical source [13]:

$$i = \frac{i_{d_s}}{1 + \sigma\delta c/\delta d} \tag{3}$$

the symbols of Equation 3 are explained at the start of this paper.

Because the electrochemically inert species S is the prevailing species in the solution ($\sigma \gg 1$) and $i_{d_s} = \sigma i_{d_o}$ (i_{d_o}–limiting diffusion current density of species O), therefore kinetic current density i is much larger than i_{d_o}. In other words, the kinetic current i is considerably larger than the limiting diffusion current density which will be observed if the chemical sources of species O were not occurring on the same surface through Reaction 1.

Replacing i_{d_s} with σi_{d_o} and i_{d_o} with $nFDC_0^*/\delta d$, we can transform Equation 3 into Equation 4 for the analysis of the experimental data:

$$1 - A'\frac{i}{\omega^{1/2}} = B\frac{i}{k_1^{1/2}} \tag{4a}$$

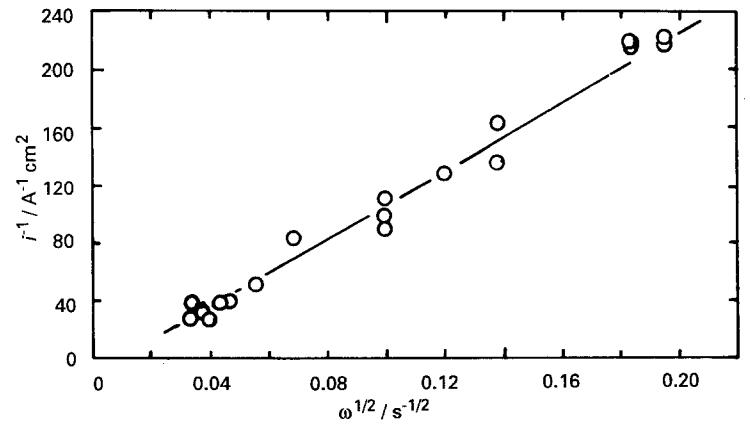

Fig. 5. Relation of $1/i$ to $1/\omega^{1/2}$.

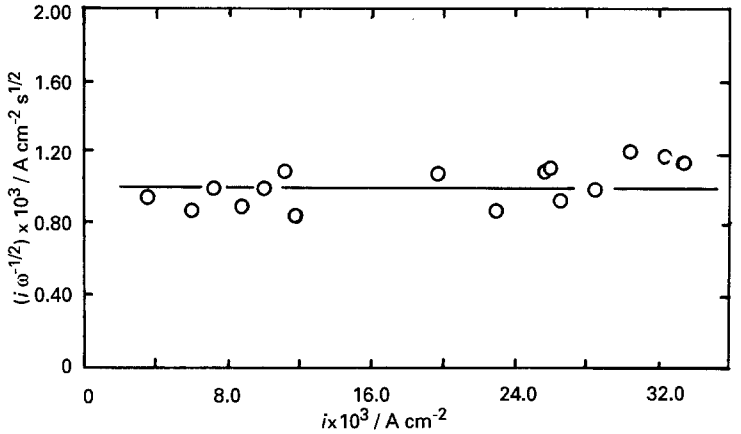

Fig. 6. Relationship between $i/\omega^{1/2}$ and i.

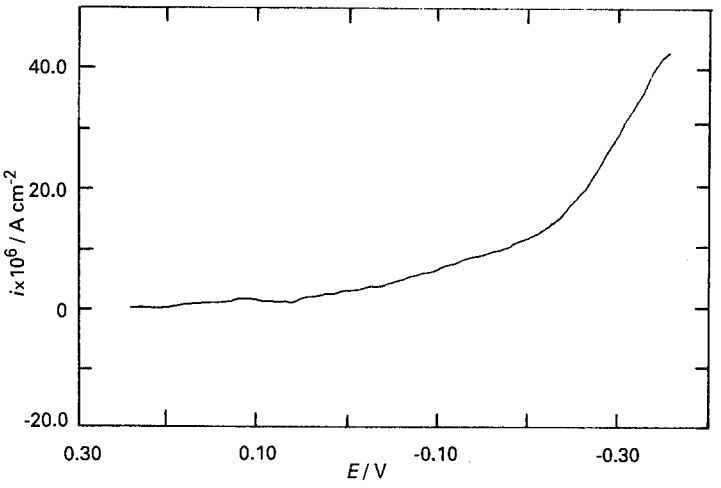

Fig. 7. Relationship between current density of hydrogen ion reduction and potential at rotating glass–carbon disc electrode. Conditions: 4 M HCl solution, RDE speed of 8000 r.p.m., and sweep rate of 1 mV s^{-1}.

or

$$\frac{i}{\omega^{1/2}} = \frac{-Bi}{A'k_1^{1/2}} + \frac{1}{A'} \qquad (4b)$$

where

$$A' = 1.61\nu^{1/6}/(nF\sigma C_0^* D^{2/3})$$

$$B = 1/(nFC_0^*\sigma^{1/2})$$

and where n is the number of electrons involved in the reaction, C_0^* is the bulk concentration of species O, and F is the Faraday constant.

The relationship of $i/(\omega)^{1/2}$ against i should be linear and the slope depends on the reaction rate of the preceding chemical reaction. As the rate increases, the slope of the line leads to zero. Figure 6 shows that the plot of $i/(\omega)^{1/2}$ against i for the antimony (III) reduction is horizontal (correlation coefficient = 0.95), which demonstrates that the preceding chemical reaction is very fast.

3.5. *Effect of antimony* (III), *hydrogen ion, and chloride ion concentration on antimony reduction*

Polarization curves under steady state at the rotating glass–carbon disc electrode with a speed of

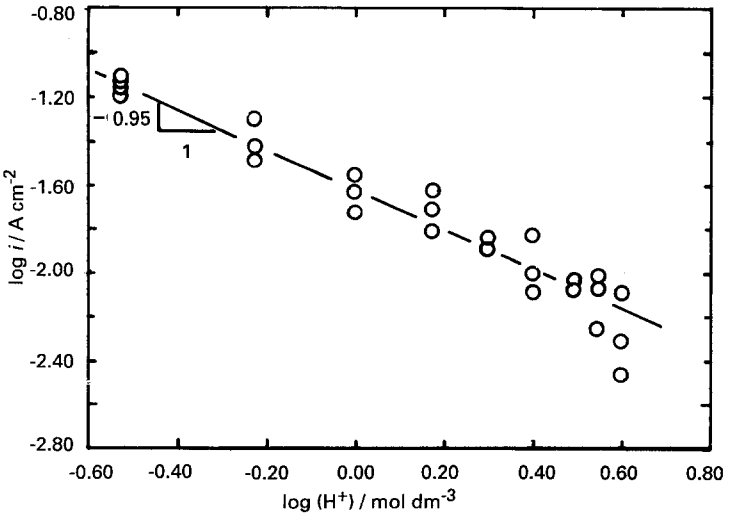

Fig. 8. Plot of log i against log (H^+) at rotating glass–carbon disc electrode of 8000 r.p.m. in the solution containing 1 g dm^{-3} Sb and 4 M Cl^-. Potential: −0.05 V vs SHE and sweep rate: 1 mV s^{-1}.

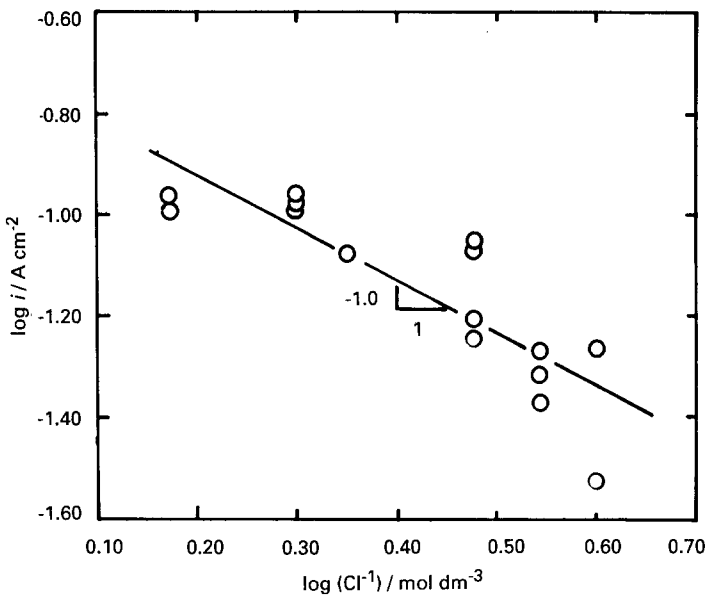

Fig. 9. Relationship between $\log i$ and $\log(Cl^-)$ at rotating glass carbon disc electrode of 8000 r.p.m. in the solution containing 1 g dm^{-3} Sb, and 0.5 M HCl. Potential: −0.05 V vs SHE and sweep rate: 1 mV s^{-1}.

8000 r.p.m. and a sweep rate of 1 mV s^{-1} were used for the study of the reaction order. Ionic strength in each series was maintained constant with the addition of sodium perchlorate.

The overpotential of hydrogen ion discharging at the glass–carbon electrode is very high and hydrogen reduction is insignificant even in the 4 M HCl solution at 8000 r.p.m. and 0.0 V (Fig. 7). Therefore, the current contributed by the H^+ reduction is negligible. Fig. 8 shows that the slope of $\log i$ against $\log[H^+]$ measured at the rotating glass–carbon electrode is −0.95 (correlation coefficient = 0.95) and the apparent reaction order with respect to $[H^+]$ is about −1. Higher acidity favours to preventing antimony (III) from electrodeposition.

The reaction order is −1.0 with respect to chloride ion concentration as indicated in Fig. 9 (correlation coefficient = 0.85). The second order reaction with respect to initial $SbCl_3$ concentration is observed at the antimony concentrations up to 1 g dm^{-3} and the zeroth order at higher antimony concentrations as indicated in Fig. 10 (correlation coefficient = 0.97).

3.6. *Adsorbing behaviour of Sb(III) species on electrode*

Potential step chronocoulometry can be used for separating the diffusion component from the adsorption and the double-layer components. In this measurement, the potentiostat applies a pulse to transfer the potential from a value where no faradaic current is flowing to a value where the surface concentration of the electrochemically active species is effectively zero.

The results of the double potential step experiment are shown in Fig. 11. The plots of total charges of the forward and reverse steps against $t^{1/2}$ and τ' respectively are given in Fig. 12, where $\tau' = \tau^{1/2} + (t-\tau)^{1/2} - t^{1/2}$.

In the forward step, the total charge Q_f, at time t, is given by [14]:

$$Q_f(t \leqslant \tau) = 2nFAC_0^* \left(\frac{D_0 t}{\pi}\right)^{1/2} + nFA\Gamma_0 + Q_{dl} \quad (5)$$

where τ is forward step duration (s), A area of glass–

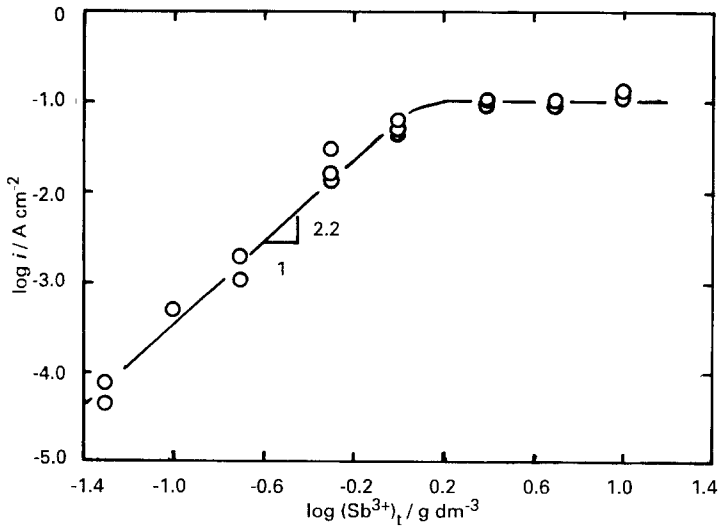

Fig. 10. Effect of total antimony (III) concentration on its cathodic process at rotating glass–carbon disc electrode of 8000 r.p.m. in the solution containing 1 M H^+, and 3.46 M Cl^-. Potential: −0.05 V vs SHE and sweep rate: 1 mV s^{-1}.

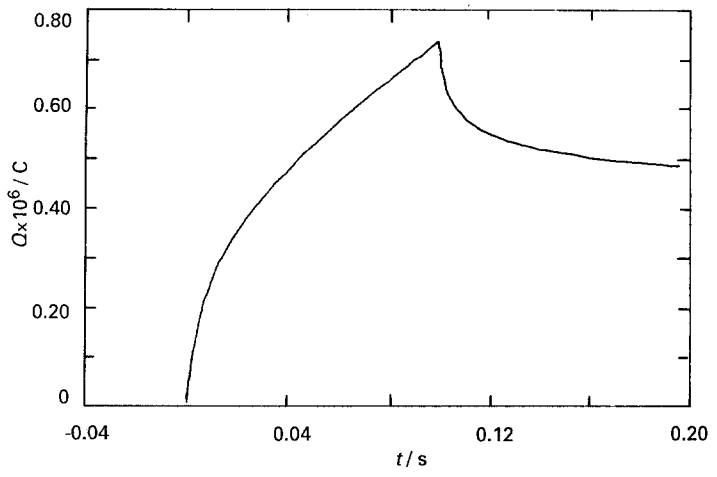

Fig. 11. Chronocoulometric response for a double-step experiment performed at glass–carbon electrode in the solution containing 1 g dm^{-3} Sb^{3+}, 0.3 M HCl and 5 M NaCl at 25° C. Initial and final potentials: 0.2415 V vs SHE, step potential −0.0185 V. Forward and reverse step durations: 0.1 s.

carbon electrode surface (cm^2), C_0^* initial bulk concentration of the electrochemically active species of Sb(III)(mol cm^{-3}), Γ_0 amount of Sb(III) species adsorbed per unit area (mol cm^{-2}), Q_{dl} charge devoted to double-layer capacitance (C), n number of electrons involved in the discharge of each ion and D_0 diffusion coefficient of the electrochemically active species of Sb (cm^2 s^{-1}).

Terms on the righthand side of Equation 5 represent the contributions from the diffusion of Sb(III) species, the adsorbed Sb(III) species and the double-layer charging, respectively. The plot of Q_f against $t^{1/2}$ (Fig. 12) yields an intercept given by

$$Q_f^0 = nFA\Gamma_0 + Q_{dl} = 0.028\,\mu C \qquad (6)$$

The charge during the reverse stop, Q_r, is given by [14]

$$Q_r(t \geqslant \tau) = 2nFAC_0^* D_0^{1/2} \pi^{-1/2} \tau' + nFA\Gamma_0 \left(1 - \frac{2}{\pi} \sin^{-1}\left(\frac{\tau}{t}\right)^{1/2}\right) + Q_{dl} \qquad (7)$$

where $\tau' = \tau^{1/2} + (t - \tau)^{1/2} - t^{1/2}$.

Equation 7 can be replaced by Equation 8 with a good approximation:

$$Q_r(t > \tau) = 2nFAC_0^* D_0^{1/2} \pi^{-1/2} \left(1 + \frac{a_1 nFA\Gamma_0}{Q_c}\right) \tau' + a_0 nFA\Gamma_0 + Q_{dl} \qquad (8)$$

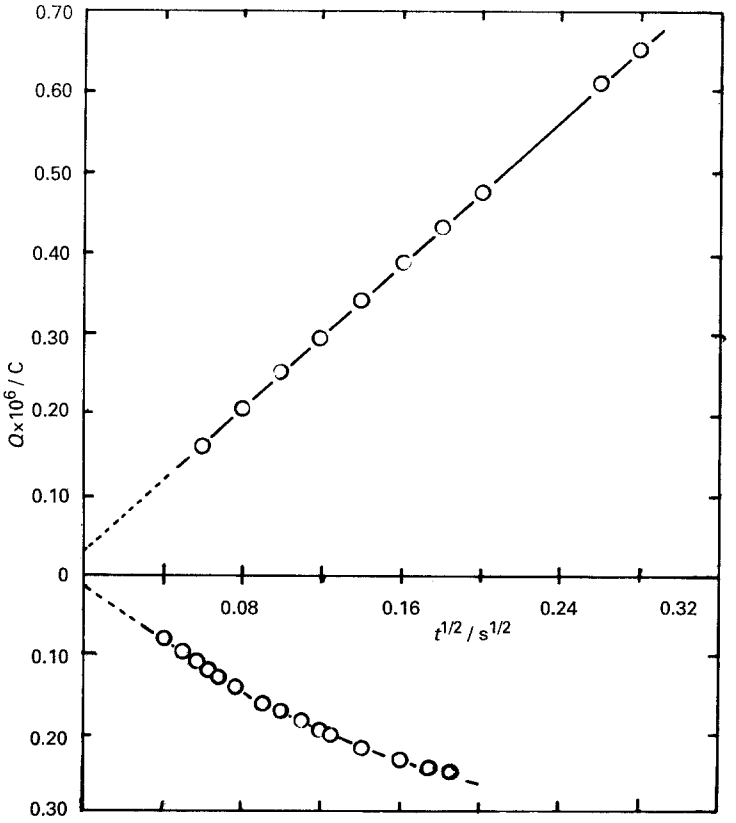

Fig. 12. Linear chronocoulometric plots based on data from Fig. 11.

where Q_c is the total charge arising from the diffusing species during the forward step. That is

$$Q_c = 2nFAC_0^* \left(\frac{D_0\tau}{\pi}\right)^{1/2} \tag{9}$$

The intercept Q_r^0 obtained from the plot of Q_r against τ' is given by

$$\begin{aligned} Q_r^0 &= a_0 nFA\Gamma_0 + Q_{dl} \\ &= a_0(Q_f^0 - Q_{dl}) + Q_{dl} \end{aligned} \tag{10}$$

The value of Q_{dl} in the presence of adsorption is thus

$$Q_{dl} = \frac{Q_r^0 - a_0 Q_f^0}{1 - a_0} \tag{11}$$

The values of a_0 and a_1 are taken as $a_0 = -0.069$ and $a_1 = 0.97$ [14], then with

$$Q_f^0 = 0.0028\,\mu C, \text{ and } Q_r^0 = 0.015\,\mu C \text{ (Fig. 11)}$$

$$Q_{dl} = \frac{0.015 + 0.069 \times 0.028}{1 + 0.069} = 0.0158\,\mu C$$

Substituting this value for Q_{dl} in Equation 6, Γ_0 can be determined to be $4.1 \times 10^{-5}\,\mu g\,cm^{-2}$.

The charge devoted to the double layer capacitance Q'_{dl} is determined experimentally to be $0.33 \times 10^{-4}\,\mu C$ in the pure supporting electrolyte solution containing no antimony. It indicates that the adsorbed Sb(III) species has a great contribution to the double layer capacitance.

3.7. *Reaction mechanism of antimony (III) reduction in chloride solutions*

Based on the results in this study, it is believed that the preceding chemical reactions exist before the discharging steps and these reactions are fast. The discharging steps display irreversibility and the degree of irreversibility increases as the sweep rate increases. Existence of some absorbate has been proved experimentally. Reaction orders of H^+, Cl^- and Sb(III) species concentration in this process have been determined to be -1, -1 and 2, respectively.

Basic antimony chloride salts may be considered as intermediate products in the cathodic process of antimony (III) chlorides. The complexation and dissociation equilibria of antimony (III) species with chloride ions surely exist. Thus, the relevant reaction mechanism can be proposed as follows:

$$SbCl_3 + H_2O \underset{k_{-12}}{\overset{k_{12}}{\rightleftharpoons}} SbOHCl_2 + H^+ + Cl^- \tag{12}$$

$$SbOHCl_2 + SbCl_3 \underset{k_{-13}}{\overset{k_{13}}{\rightleftharpoons}} Sb_2OHCl_5(\text{adsorbate}) \tag{13}$$

$$Sb_2OHCl_5(\text{adsorbate}) + e^- \xrightarrow{k_{14}} Sb_2OHCl_4(\text{adsorbate}) + Cl^- \tag{14}$$

$$Sb_2OHCl_4(\text{adsorbate}) + e^- \underset{k_{-15}}{\overset{k_{15}}{\rightleftharpoons}} Sb_2OHCl_3(\text{adsorbate}) + Cl^- \tag{15}$$

$$Sb_2OHCl_3(\text{adsorbate}) + H^+ + e^- \underset{k_{-16}}{\overset{k_{16}}{\rightleftharpoons}} Sb + SbCl_3 + H_2O \tag{16}$$

Reaction 12 is fast and in equilibrium all the time, then

$$\frac{[SbOHCl_2][H^+][Cl^-]}{[SbCl_3]} = \frac{k_{12}}{k_{-12}} = K_{12} \tag{17}$$

Reaction 13 is also fast. Let the fraction of the adsorption sites on the electrode surface covered by the adsorbate, Sb_2OHCl_5, at a given time be θ. Reaction 14 is slow and hence the rate determining step and the subsequent reactions (15–16) are fast which do not affect the rate of process. Then the change rate of θ with time is

$$\frac{d\theta}{dt} = k_{13}[SbOHCl_2][SbCl_3](1 - \theta) - k_{-13}\theta - k_{14}\theta \tag{18}$$

At steady state, $d\theta/dt = 0$, and Equation 18 reduces to

$$\theta = \frac{k_{13}[SbCl_3][SbOHCl_2]}{k_{13}[SbCl_3][SbOHCl_2] + k_{-13} + k_{14}} \tag{19}$$

Substituting Equation 17 into Equation 19, Equation 20 is obtained:

$$\theta = \frac{k_{13}K_{12}[SbCl_3]^2/[H^+][Cl^-]}{k_{13}K_{12}[SbCl_3]^2/[H^+][Cl^-] + k_{-13} + k_{14}} \tag{20}$$

The overall rate of the process is controlled by the slowest reaction (14), thus the cathodic current with three electrons discharging is

$$I = 3AFk_{14}\theta = \frac{3AFK_{12}k_{13}k_{14}[SbCl_3]^2/[H^+][Cl^-]}{K_{12}k_{13}[SbCl_3]^2/[H^+][Cl^-] + k_{-13} + k_{14}} \tag{21}$$

where:

K_{12} equilibrium constant of Reaction 12,
k_{13}, k_{-13} rate constants of forward and backward reactions of Equation 13, respectively,
k_{14} rate constant of Reaction 14, and
A electrode surface area

At low concentrations of Sb(III) species, the first term in the denominator of Equation 21 is negligible, then the equation reduces to

$$I = \frac{3AFK_{12}k_{13}k_{14}}{k_{-13} + k_{14}} \frac{[SbCl_3]^2}{[H^+][Cl^-]} \tag{22}$$

It displays that reaction orders with respect to $[SbCl_3]$, $[H^+]$ and $[Cl^-]$ are 2, -1 and -1, respectively, which are consistent with the experimental results.

On the contrary, at the higher concentration of Sb(III) species, the first term in the denominator of Equation 21 may become dominant and the reaction order with respect to $[SbCl_3]$ leads to zero, which is confirmed by experiment results indicated in Fig. 10.

With a similar derivation, different reaction orders with respect to $[SbCl_3]$, $[H^+]$ and $[Cl^-]$

will result: if other steps were rate determining. Furthermore, changes on Reaction 12, 13 or 14 will also result in different reaction orders in the rate equation.

4. Summary and conclusions

The reaction mechanism of the cathodic reaction of Sb(III) species in chloride solutions (Reactions 12–16) is proposed based on the experimental results. The mechanism explains satisfactorily all experimental results in this study. The results are summarized as below:

(i) Preceding chemical reactions (Reactions 12 and 13) occur on the cathode surface before the discharging step (Reaction 14). This phenomenon is evidenced by the results obtained with cyclic voltammetry and rotating disc electrode technique and these reactions are demonstrated to be fast.

(ii) Adsorption of antimony species on the electrode is clearly demonstrated by using potential step chronocoulometry.

(iii) A.c. impedance measurements indicate the reduction of antimony species is not a simple charge transfer reaction.

(iv) By using cyclic voltammetry technique, the discharging step (Reaction 14) is shown to be irreversible.

(v) At low antimony concentrations, the reaction orders of the reduction of antimony species with respect to the concentrations of antimony, hydrogen and chloride ions are determined to be 2, −1 and 1, respectively by applying the cyclic sweep on the rotating disc electrode. These measured reaction orders corrolorate the rate equation (Equation 22) which is derived from the proposed mechanism.

Acknowledgments

The authors wish to express their appreciation to Nerco Minerals Company for financial support and permission to publish this paper.

References

[1] Sumitomo Metal Mining Co., Ltd, Removal of antimony from copper electrorefining bath. *Japanese Kokai: Tokkyo Koho JP 57 155 399 (82 155 399)* 25 Sept. (1982) 4 pp.

[2] Nippon Mining Co., Ltd, Removal of bismuth and antimony from aqueous sulfuric acid acidic solutions, *Japanese Kokai: Tokkyo Koho JP 59 208 089 (84 208 089)* 26 Nov. (1984) 3 pp.

[3] M. Ishiwatari and E. Kimura, A method for treating a sulfuric acid acidic solution containing antimony and bismuth, *Japanese Kokai: Tokkyo Koho JP 62 260 090 (87 260 090)* 12 Nov. (1987) 3 pp.

[4] D. M. Muir and G. Senanayake, 'Principles and Applications of Strong Salt Solutions to Mineral Chemistry', Extraction Metallurgy '86, The Institution of Mining and Metallurgy, London (1985) pp. 65–91.

[5] F. E. Lamb, Hydrometallurgy production of antimony, *US Patent 3 986 943*, 19 Oct. (1976) 14 pp.

[6] G. Su, 'New Hydrometallurgical Process for Antimony', A Research Report of Hunan Metallurgical Research Institute, China (1981).

[7] X. Xu, D. Zheng and C. Fu, 'Fundamental Studies on the Hydrometallurgy of Antimony – XPS Studies on Chloride in Explosive Antimony', Zhougnan Kuangye Xueyuan Xuebao (1987) 18(1), pp. 31.

[8] X. Xu, 'Mechanism of and Conditions for the Formation of Explosive Antimony', Master's thesis, Central South Institute of Mining and Metallurgy, China (1984).

[9] R. S. Nicholson and I. Shain, *Anal. Chem.* **36** (1964) 706.

[10] D. D. MacDonald, 'Transient Techniques in Electrochemistry', Plenum Press, New York (1977) pp. 195–201.

[11] V. G. Levich, 'Physiochemical Hydrodynamics', Prentice-Hall, Englewood Cliffs, NJ (1962).

[12] Z. Tian, Researching Methods of Electrochemistry, Scientific Publisher Sinica, Beijing (1981) pp. 80–102.

[13] Yu V. Pleskov and V. Yu. Filinvskii, 'Vrasbshayusbshii Diskovyi Electrod', Izdatel'stva Nauka, Moskova (1972) pp. 74–99.

[14] A. J. Bard and L. R. Faulkner, 'Electrochemical Methods', John Wiley & Sons, New York (1980) pp. 535–538.